Chemo-Dynamical Galaxy Evolution

Matthias Kühtreiber [1]
Gerhard Hensler, Rainer Spurzem, Peter Berczik, Lei Liu,
The Silkroad-Project Team

[1] Department of Astrophysics, University of Vienna

December 20, 2016

Outline

Dwarf Galaxies: Definition

Properties

- Low-luminosity: $M_v \geq 10^{-17}$ mag
- Low-mass: $10^7 - 10^{10} \mathrm{M}_\odot$
- Small in size: a few kpc
- Often low surface brightness, so they are hard to find

There are different types of dwarf galaxies:

- Dwarf irregulars (dIrr): Gas-rich, active ongoing star formation but relatively low surface brightness;
- Dwarf ellipticals (dEs): Gas-poor, old stellar population, many dEs show nuclei and are structurally different from luminous elliptical galaxies;
- Dwarf spheroidals (dSph): Gas-poor, extremely low luminosity;

IC 2574: dIrr

M 110: dE

Leo I: dSph

Dwarf Galaxies

universität wien

Absolute magnitude M_v vs. central surface brightness μ_v:

- ⬠ Local group dwarf galaxies
- ■ Blue compact dwarf galaxies
- △ Milky Way, M31, M33, LMC

- dEs and dIrrs follow the same relation, even to the very faint end.
- But clearly distinct from ultra compact dwarfs (UCDs), globular clusters (GCs) and Hubble type galaxies

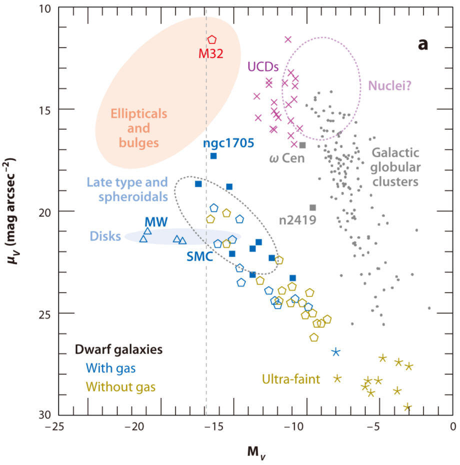

Tolstoy et al. (2009); reproduced by Liu Lei

Why are dwarf galaxies interesting?

Dwarf galaxies

- are the most common class of galaxies.
- are relatively simple systems, not merger products.
- are currently being "absorbed" by larger galaxies (hierarchical formation).
- are extremely sensitive to their internal evolution and their environmental influences.

Metallicity

- DGs have usually low metallicities
- DGs follow a metallicity luminosity relation but dIrrs and dEs/dSphs follow different tracks
- Galactic outflows might be one cause for low metallicities
- Observations show different abundances for neutral/ionized gas
- Multi-Phase treatment for a more realistic chemo-dynamical evolution!

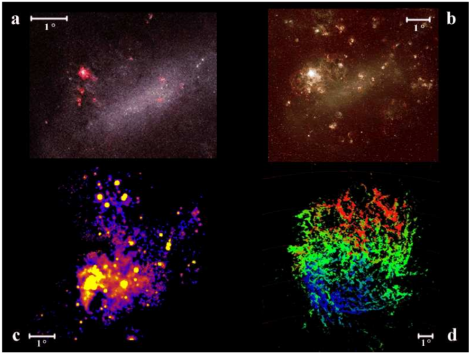

Figure 1. The dwarf irregular galaxy *Large Magellanic Cloud* (LMC) at different wavelengths: a) optical image showing stars and luminous interstellar gas; b) $H\alpha$ image pronouncing star forming regions; c) X-ray here traces hot supernova expelled gas; d) large-scale neutral hydrogen gas structures in the 21 cm radio line. Please note the different scales of the four images.

The Interstellar Medium

For heating-cooling balance 3 stable phases can form.

$$n^2\Lambda(T) = nG$$

$$\frac{\Lambda(T)}{T} = \frac{G}{nT}$$

- Cold medium: molecular clouds; $T \sim 100$ K; $n \sim 10^2 - 10^6$ cm^{-3}
- Warm partly ionized medium: $T \sim 10^4$ K; $n \sim 0.1$ - a few cm^{-3}
- hot gas: $T \sim 10^6$ K; $n \sim 10^{-1} - 10^{-3}$ cm^{-3}

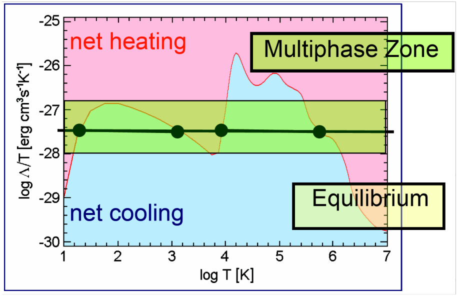

Credit: Günter Hasinger

The Multi-Phase Model

universität wien

"Sticky" particle method by Theis & Hensler (1993)

Hot/Warm Component

- SPH particles
- Can condensate ⇒ cold clouds
- Receive feedback from SNII and SNIa

Cold Clouds

- N-body particles
- Can coagulate due to collisions
- Can form stars and fragment
- Can evaporate ⇒ hot/warm component
- Receive stellar wind and PNe feedback

The hot/warm and cold component can exchange mass, momentum and energy due to:

- condensation
- evaporation
- drag force

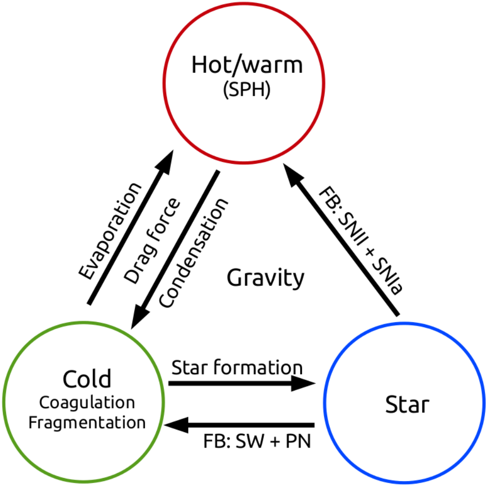

Hot Gas

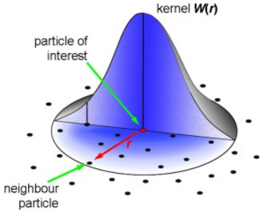

$$W(r;h) = \frac{1}{\pi h^3} \begin{cases} 1 - \frac{3}{2}\left(\frac{r}{h}\right)^2 + \frac{3}{4}\left(\frac{r}{h}\right)^3, & \text{for } 0 \le \frac{r}{h} \le 1, \\ \frac{1}{4}\left(2 - \frac{r}{h}\right)^3, & \text{for } 1 \le \frac{r}{h} \le 2, \\ 0, & \text{for } \frac{r}{h} > 2. \end{cases}$$

- The fluid is divided into a set of discrete elements (particles)
- A smoothing length h is applied to particles
- Properties are smoothed between neighbouring particles via a kernel function $W\left(\vec{r_{ij}}, h\right)$

Field F is known at some points $\vec{r}$: $F = F(\vec{r})$
The smoothed interpolated version of F is defined as

$$F_s(\vec{r}) = \int F(\vec{r}) W(\vec{r} - \vec{r'}, h) d\vec{r'}$$

Can be approximated by a sum:

$$F_s(\vec{r}) \simeq \sum_j \frac{m_j}{\rho_j} F(\vec{r_j}) W(\vec{r} - \vec{r_j}, h)$$

$$\rho_i = \sum_j m_j W(\vec{r_i} - \vec{r_j}, h)$$

Smoothed Particle Hydrodynamics (SPH)

Equation of motion and internal energy:

$$\frac{d\mathbf{v}_i}{dt} = -\sum_j m_j \left(\frac{P_i}{\rho_i^2} + \frac{P_j}{\rho_j^2} + \Pi_{ij} \right) \nabla_i W_{ij}$$

$$\frac{du_i}{dt} = \frac{1}{2} \sum_j m_j \left(\frac{P_i}{\rho_i^2} + \frac{P_j}{\rho_j^2} + \Pi_{ij} \right) (\mathbf{v}_i - \mathbf{v}_j) \nabla_i W_{ij}$$

$P\ldots$ pressure $= (\gamma - 1) \cdot \rho_i \cdot u_i$
$\Pi_{ij}\ldots$ artificial viscosity
$c_{ij}\ldots$ mean sound speed $= (c_i + c_j)/2$
$\epsilon = 0.01$
$f_{ij} = (f_i + f_j)/2$

Artificial viscosity:

$$\Pi_{ij} = \begin{cases} \frac{-\alpha c_{ij}\mu_{ij} + \beta\mu_{ij}^2}{\rho_{ij}} & \mathbf{v}_{ij} \cdot \mathbf{r}_{ij} < 0, \\ 0 & \text{else} \end{cases}$$

$$\mu_{ij} = \frac{h_{ij}(\mathbf{v}_i - \mathbf{v}_j) \cdot (\mathbf{r}_i - \mathbf{r}_j)}{\mathbf{r}_{ij}^2 + \epsilon h_{ij}^2} f_{ij}$$

$$f_i = \frac{|(\nabla \cdot \mathbf{v})_i|}{|(\nabla \cdot \mathbf{v})_i| + |(\nabla \times \mathbf{v})_i| + \epsilon^2 c_i / h_i}$$

Cold Clouds

Size of the cloud is calculated by mass-radius relation Larson (1981), Rivolo (1988):

$$h_{\mathrm{cl}} = 50\sqrt{\frac{m_{\mathrm{cl}}}{10^6\ \mathrm{M}_\odot}}(\mathrm{pc})$$

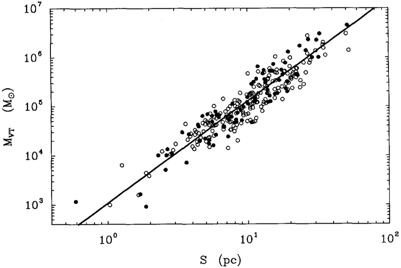

Figure 3. Mass–radius relation for 273 giant molecular clouds from the catalog of Solomon *et al.* (1987). The solid circles are calibrator clouds with known distances. The fit line is given by $M_{VT} = 330\ S^{1.97}\ M_\odot$.

Cold Clouds

Alternative: Pressureequilibrium with surrounding intercloud medium

$$h_{\mathrm{cl}} = \left(\frac{3 n_{mol} R_{gas} T}{4 \pi P} \right)^{\frac{1}{3}}$$

$$P_i = \sum_j (\gamma - 1) m_j u_j W_{ij}$$

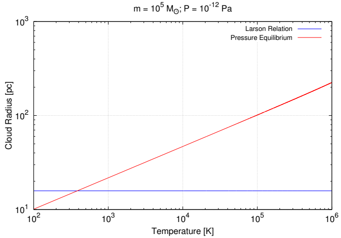

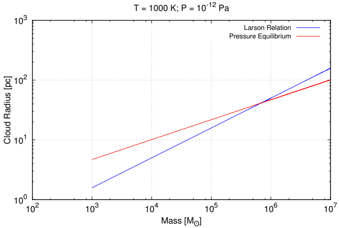

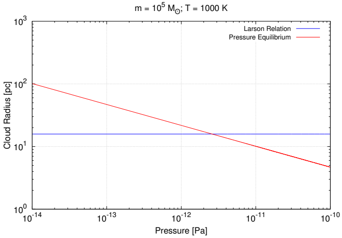

Coagulation

Theis & Hensler (1993)

1. Find clouds j around target cloud i within radius $r_{s,p}$

Typical distance travelled within next timestep

$$r_{s,p} = 2\Delta t \sqrt{2} v_{\mathrm{vir},p} = \Delta t \sqrt{8/3\phi_p}$$

Δt... next timestep;
ϕ_p... gravity potential on position of particle p

2. Linear extrapolation of the orbits to check if the separation becomes less then the sum of the cross-sections

Colisional cross-section

$$A_{\mathrm{cr}} = \eta_{\mathrm{ov}}^2 \cdot \pi h_{\mathrm{cl}}^2 \cdot \left(1 + \frac{2G(m_1 + m_2)}{\eta_{\mathrm{ov}} h_{\mathrm{cl}} v_{1,2}^2}\right)$$

$\eta_{\mathrm{ov}} = 0.2$;

3. Check critical spin of compound object

Critical spin

$$m_1 m_2/(m_1 + m_2) \cdot b\, v_{1,2} \leq c_{\mathrm{ang}} L_{\mathrm{max}}$$

$$L_{\mathrm{max}} = \int \rho(\mathbf{r}) v_{\mathrm{circ}}\, r \sin\theta \, \mathrm{d}\mathbf{r} = \frac{8}{21} \cdot \sqrt{G m_{\mathrm{cl}}^3 h_{\mathrm{cl}}}.$$

b... impact parameter
$c_{\mathrm{ang}} = 1$
θ... angle between rotation axis and position r

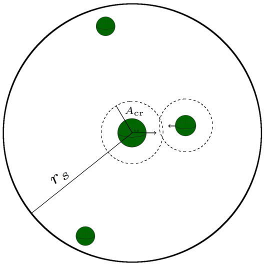

Fragmentation

- Triggered by stellar feedback: SW and SNeII drive an expanding shell
- The radius r_{sh} and velocity v_{sh} of the shell are determined by:

Expanding Shell

$$r_{\rm sh} = 0.961 \cdot \left(\frac{\dot{E}}{\rho_1}\right)^{0.25} \cdot t^{\,0.75}$$

$$v_{\rm sh} = 0.736 \cdot \left(\frac{\dot{E}}{\rho_1}\right)^{0.25} \cdot t^{\,-0.25}$$

$\rho_1 ... m_{cl}/h_{cl}^{(3-\alpha)}$; α...determines $\rho(r)$ of a cloud from mass-radius relation follows $\alpha = 1$

- When r_{sh} reaches the edge of the cloud, it fragments into 4 smaller pieces.
- The fragments get the velocity of the expanding shell v_{sh} at that time.

Brown et al. (1995)

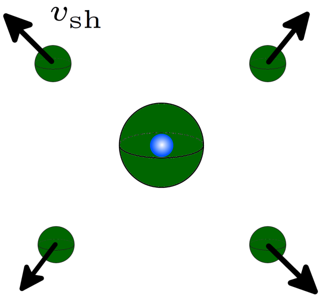

Thermal Conduction

- Analytical formulae by Cowie et al. (1981)
- Leads to evaporation and condensation of clouds
- σ_0 represents the ratio between the electron mean free path λ_k and the cloud size h_{cl}:

Thermal Conduction

$$\sigma_0 = \left(\frac{T_{\mathrm{hot}}(\mathrm{K})}{1.54\times 10^7}\right)^2 \frac{1}{\Phi\, n_{\mathrm{hot}}(\mathrm{cm}^{-3})\, h_{\mathrm{cl}}(\mathrm{pc})}$$

T_{hot}... Temperature of hot/warm gas;
n_{hot}... number density of hot/warm gas;
Φ... Effect of a magnetic field on reducing the mean free path of charged particles (is set to 1);

- If $h_{cl} < \lambda_k$ ($\sigma_0 > 1$) $\Rightarrow$ evaporation occurs
- If $h_{cl} > \lambda_k$ $\Rightarrow$ condensation occurs
- The transition value from evaporation to condensation is set to $\sigma_0 = 0.03$

Condensation/Evaporation

$$\frac{\mathrm{d}m_{\mathrm{cl}}}{\mathrm{d}t}(\mathrm{kg/s}) = \begin{cases} 0.825\cdot T_{\mathrm{hot}}^{5/2} h_{\mathrm{cl}}\sigma_0^{-1} & \sigma_0 < 0.03 \\ -27.5\cdot T_{\mathrm{hot}}^{5/2} h_{\mathrm{cl}}\Phi & 0.03 \le \sigma_0 \le 1 \\ -27.5\cdot T_{\mathrm{hot}}^{5/2} h_{\mathrm{cl}}\Phi\sigma_0^{-5/8} & \sigma_0 > 1 \end{cases}$$

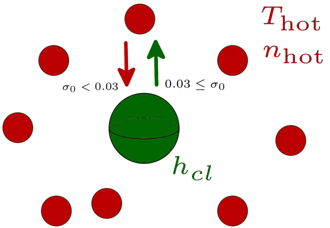

Thermal Conduction

$$\Delta m_{cl} = \frac{dm_{cl}}{dt} \cdot \Delta t_{CE}; \quad m'_{cl} = m_{cl} + \Delta m_{cl}; \quad m'_{hot} = m_{hot} + \Delta m_{cl};$$

Momentum Exchange

$$M_{hot} \cdot \mathbf{v}_{hot} + m_{cl} \cdot \mathbf{v}_{cl} = m'_{hot} \cdot \mathbf{v}'_{hot} + m'_{cl} \cdot \mathbf{v}'_{cl}$$

$$M'_{hot} = m_{hot} - \Delta m_{cl}$$

$$M'_{cl} = m_{cl} + \Delta m_{cl}$$

If $\Delta m_{cl} > 0$: condensation
If $\Delta m_{cl} < 0$: evaporation

Temperature Exchange

Condensation: $T'_{hot} = T_{hot}$

$$(m_{cl} + \Delta m_{cl}) \cdot T'_{cl} = m_{cl} \cdot T_{cl} + \Delta m_{cl} \cdot T_{hot}$$

$$T'_{cl} = \frac{m_{cl} \cdot T_{cl} + \Delta m_{cl} \cdot T_{hot}}{m_{cl} + \Delta m_{cl}}$$

Evaporation: $T'_{cl} = T_{cl}$

$$(m_{hot} - \Delta m_{cl}) \cdot T'_{hot} = m_{hot} \cdot T_{hot} - \Delta m_{cl} \cdot T_{cl}$$

$$T'_{hot} = \frac{m_{hot} \cdot T_{hot} - \Delta m_{cl} \cdot T_{cl}}{m_{hot} - \Delta m_{cl}}$$

Cloud Dragging

universität wien

- Different dynamics lead to a drag force acting on clouds
- Analytical formulae by Shu et al. (1972)

Drag Force

$$\mathbf{F}_{\mathrm{D}} = -C_{\mathrm{D}} \cdot \pi h_{\mathrm{cl}}^2 \, \rho_{\mathrm{hot}} \cdot |\mathbf{v}_{\mathrm{cl}} - \mathbf{v}_{\mathrm{hot}}| \cdot (\mathbf{v}_{\mathrm{cl}} - \mathbf{v}_{\mathrm{hot}}).$$

C_{D}... Ratio between the effective cross section of a cloud and its geometrical one (πh_{cl}^2);
$\mathbf{v}_{\mathrm{cl}} - \mathbf{v}_{\mathrm{hot}}$... Relative velocity of the cloud in a homogeneous surrounding hot medium;

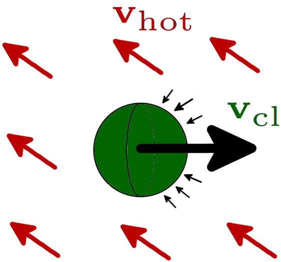

Gas Cooling

universität wien

- $T > 10^4$ K: continuum emission and line emission
  Böhringer & Hensler (1989)
- $T < 10^4$ K: thermal collisions (Dalgarno & McCray 1972)
  and contribution of H_2 and HD
  Hollenbach & McKee (1979) and
  Lipovka et al. (2005)

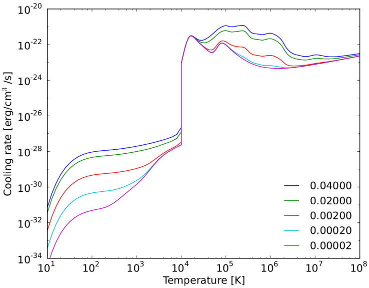

$$\Lambda(T,Z)_{T<10^4} = \underbrace{n_H^2 f_i \Lambda_{e^-}(T,Z)}_{\text{collis. with e}^-} + \underbrace{n_H^2 \Lambda_{Atom}(T,Z)}_{\text{collis. with neutral H}} + \underbrace{n_{tot}^2 \Lambda_{Molec.}(T)}_{\text{molecules}},$$

$$\Lambda(T,Z)_{T>10^4} = n_H^2 f_i \Lambda_{e^-}(T,Z)$$

- Jeans instability criterion can directly be used
- Check if $\lambda_{\mathrm{J}} < h_{cl} \Rightarrow$ collapse

$$\lambda_{\mathrm{J}} \equiv c_{\mathrm{cl}} \sqrt{\frac{\pi}{G\rho_{\mathrm{cl}}}}$$

$$\frac{\mathrm{d}\rho_*^{\max}}{\mathrm{d}t} = \frac{M_{\mathrm{J}}}{\tau_{\mathrm{cl}}^{\mathrm{ff}} V_{\mathrm{J}}} = \frac{4}{3}\sqrt{\frac{6G}{\pi}}\ \rho_{\mathrm{cl}}^{3/2}$$

$$\tau_{\mathrm{cl}}^{\mathrm{ff}} \equiv \sqrt{\frac{3\pi}{32G\rho_{\mathrm{cl}}}}$$

- $\mathrm{d}\rho_*^{\max}/\mathrm{d}t$ is multiplied with a random number ϵ between 0.01 and 1 because usually not the total mass M_J is turned into stars within a free-fall time $\tau_{\mathrm{cl}}^{\mathrm{ff}}$

$$\frac{\mathrm{d}\rho_*}{\mathrm{d}t} = \epsilon \cdot \frac{\mathrm{d}\rho_*^{\max}}{\mathrm{d}t}$$

Single Stellar Populations

Initial mass function from Kroupa et al. (1993), with $m_{low} = 0.08\ M_\odot$ and $m_{up} = 100\ M_\odot$

$$\xi(m) = \begin{cases} 0.035 m^{-1.3} \text{ if } & 0.08 \leq m < 0.5, \\ 0.019 m^{-2.2} \text{ if } & 0.5 \leq m < 1.0, \\ 0.019 m^{-2.7} \text{ if } & 1.0 \leq m < 100 \end{cases}$$

Stellar lifetimes from Raiteri et al. (1996):

$$\log t_\star = a_0(Z) + a_1(Z)\log M + a_2(Z)(\log M)^2$$

$$a_0(Z) = 10.13 + 0.07547 \log Z - 0.008084(\log Z)^2$$
$$a_1(Z) = -4.424 - 0.7939 \log Z - 0.1187(\log Z)^2$$
$$a_2(Z) = 1.262 + 0.3385 \log Z + 0.05417(\log Z)^2$$

- High mass stars: $M > 8\ M_\odot$ Produce stellar winds and end their life as SNeII
- Intermediate mass stars: $0.8\ M_\odot > M > 8\ M_\odot$ Undergo PNe or SNeIa
- Low mass stars: $M < 8\ M_\odot$ Do not evolve significantly during a Hubble time

Feedback

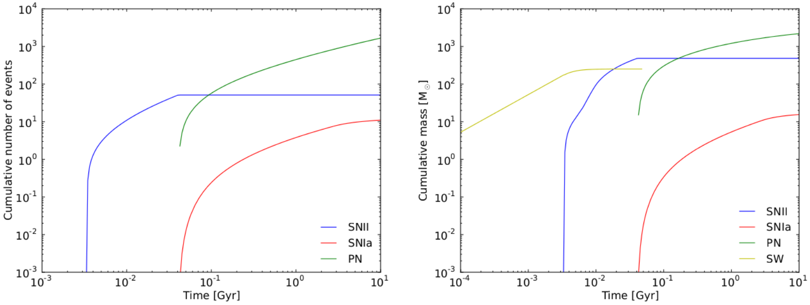

- Stellar particles return mass, energy and chemical elements to surrounding hot and cold particles
- Feedback from SNe is added to the hot phase
- Feedback from SW and PNe is added to the cold phase
- Mass ejecta are calculated from models of Berczik & Petrov (2003)

Yields

- SW & SNII: Portinari et al. (1998)
- PNe: van den Hoek & Groenwegen (1997)
- SNIa: Iwamoto et al. (1999)

Feedback

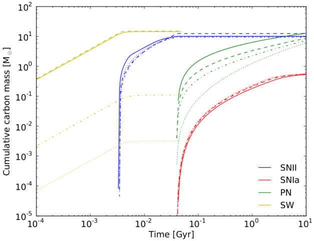

Carbon

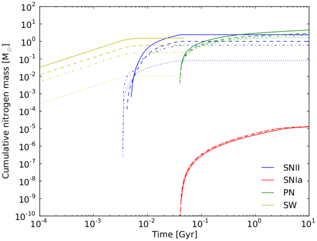

Nitrogen

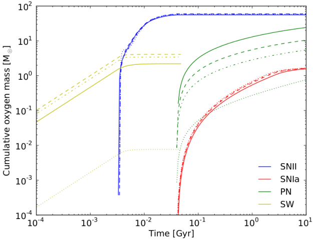

Oxygen

Z = 0.02, 0.008, 0.004, 0.0004

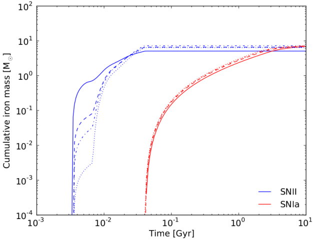

Iron

Feedback

Feedback energy ΔE of a SSP in the time interval $[t, t + dt]$:

$$\Delta E = [\Delta E_{\mathsf{SW}}(t) + \Delta N_{\mathsf{PN}}(t) E_{\mathsf{PN}} + (\Delta N_{\mathsf{SNII}}(t) E_{\mathsf{SNII}} + \Delta N_{\mathsf{SNI}}(t) E_{\mathsf{SNI}}) \cdot SN_{\mathsf{eff}}]\, m_\star$$

$$E_{\mathsf{PN}} = 10^{47} \mathsf{erg}$$
$$E_{\mathsf{SNII}} = 10^{51} \mathsf{erg}$$
$$E_{\mathsf{SNI}} = 10^{51} \mathsf{erg}$$
$$SN_{\mathsf{eff}} = 0.05$$

Mass transfer of a SSP in the time interval $[t, t + dt]$:

$$\Delta m(t) = [\Delta m_{PN}(t) + \Delta m_{SNII}(t) + \Delta m_{SNI}(t) + \Delta m_{SW}(t)] m_\star$$

11 elements are taken into account: H, He, C, N, O, Ne, Mg, Si, S, Ca, Fe

$$\Delta m_k(t, Z) = [\Delta m_{k,PN}(t, Z) + \Delta m_{k,SNII}(t, Z) + \Delta m_{k,SNI}(t, Z) + \Delta m_{k,SW}(t, Z)] m_\star$$

N ... number of events $m_\star$ ... mass of stellar population Δm... feedback mass
Δm_k ... feedback mass for element k

Mass Transfer

Star Formation:

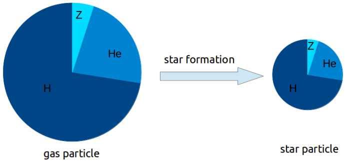

$$m_{gas} = m_{gas} - m_{star}$$

$$m_{k,star} = \frac{m_{k,gas}}{m_{gas}} m_{star}$$

$$m_{k,gas} = m_{k,gas} - m_{k,star}$$

Feedback: H, He, C, N, O, Ne, Mg, Si, S, Ca, Fe

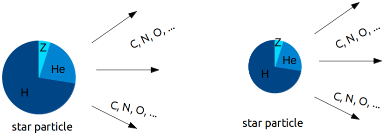

$$m_{star} = m_{star} - \Delta m(t)$$

$$m_{k,star} = m_{k,star} - \Delta m(t) \frac{m_{k,star}}{m_{star}}$$

$$m_{gas} = m_{gas} + \Delta m(t) * frac$$

$$m_{k,gas} = m_{k,gas} + \Delta m_k(t) * frac$$

Δm... feedback mass Δm_k ... feedback mass for element k m_{star} ... mass of stellar population

frac ... feedback fraction one of the neighbouring gas particles receives (e.g. $W(r_{i,j}, h)$ or N_{ngb})

Initial Conditions

Gas

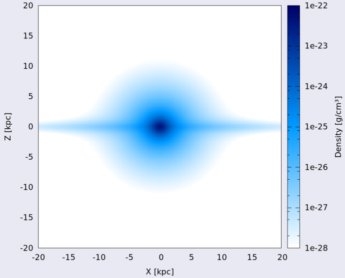

- Miyamoto-Nagai profile with $a = 0.2$ kpc and $b = 0.75$ kpc
- Hot/warm: $M = 4 \times 10^7$ M$_\odot$, $T = 10^6$ K
- Cold: $M = 1.96 \times 10^9$ M$_\odot$, $T = 10^3$ K

$\Rightarrow \mathbf{M_{gas} = 2 \times 10^9}$ M$_\odot$

Dark Matter

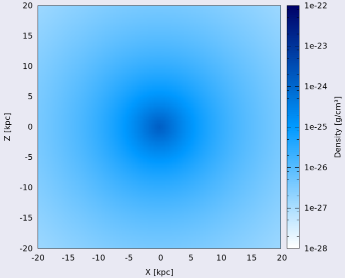

- Burkert profile with $r_0 = 3$ kpc and $\rho_0 = 1.49 \cdot 10^{-24}$ g cm^{-3}
- $\Rightarrow \mathbf{M_{dm} = 9.42 \times 10^9}$ M$_\odot$ within 20 kpc

"dw26": Option SplitHot is enabled; $M_{warm,min} = 5 \times 10^{-3}$ M$_\odot$; $M_{warm,max} = 8 \times 10^{3}$ M$_\odot$

h_{min} [kpc]	h_{max} [kpc]	ϵ [kpc]	dt_{min} [Myr]	dt_{max} [Myr]	C_{drag} -	r_{ce} [kpc]	C_{coll} -	dt_{coll} [Myr]
10^{-2}	5	0.5	10^{-2}	10^{-1}	1	1	10^{-2}	8×10^{3}

N_{hot} -	N_{cold} -	M_{hot} [M$_\odot$]	M_{cold} [M$_\odot$]	T_{hot} $[K]$	T_{cold} $[K]$
499995	50000	4×10^{7}	1.96×10^{9}	10^{5}	10^{3}

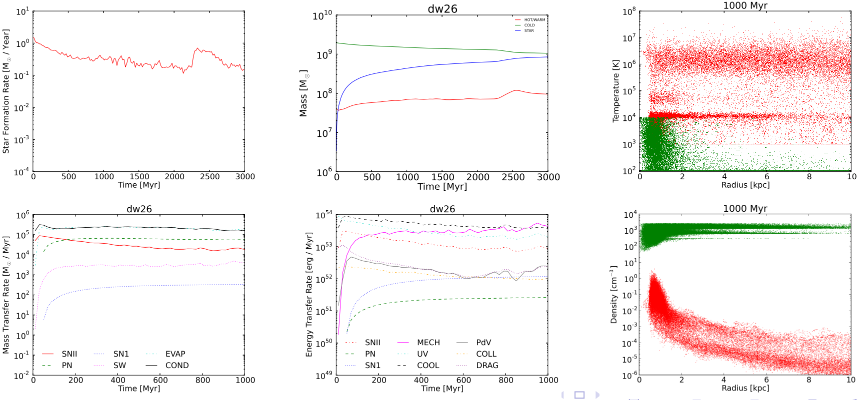

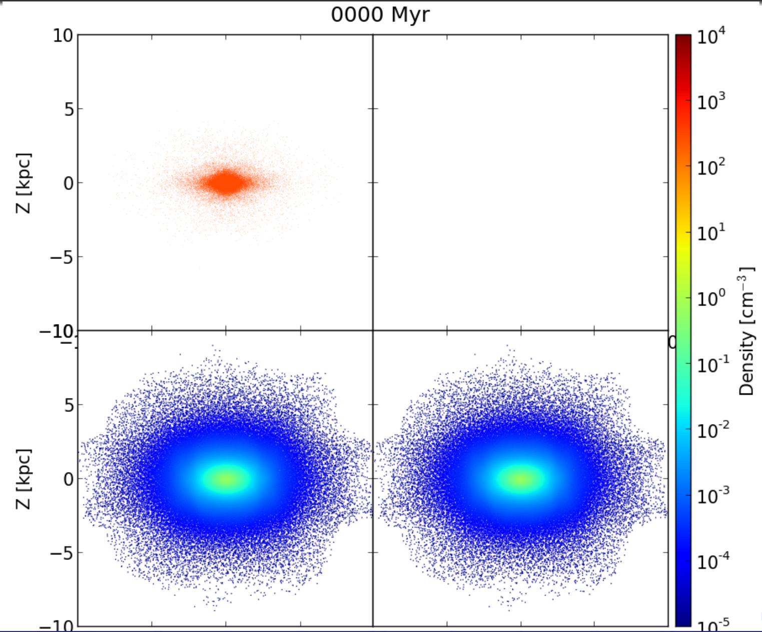
0000 Myr
Z [kpc]
10
5
0
−5
−10
Density [cm^{-3}]
10^4
10^3
10^2
10^1
10^0
10^{-1}
10^{-2}
10^{-3}
10^{-4}
10^{-5}

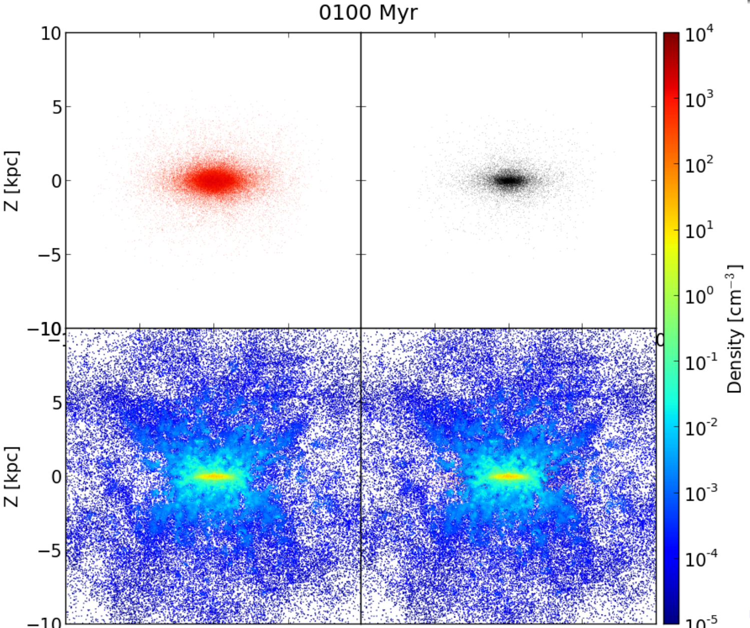
0100 Myr
Z [kpc]
Z [kpc]
10
5
0
−5
−10
10^4
10^3
10^2
10^1
10^0
10^-1
10^-2
10^-3
10^-4
10^-5
Density [cm^-3]

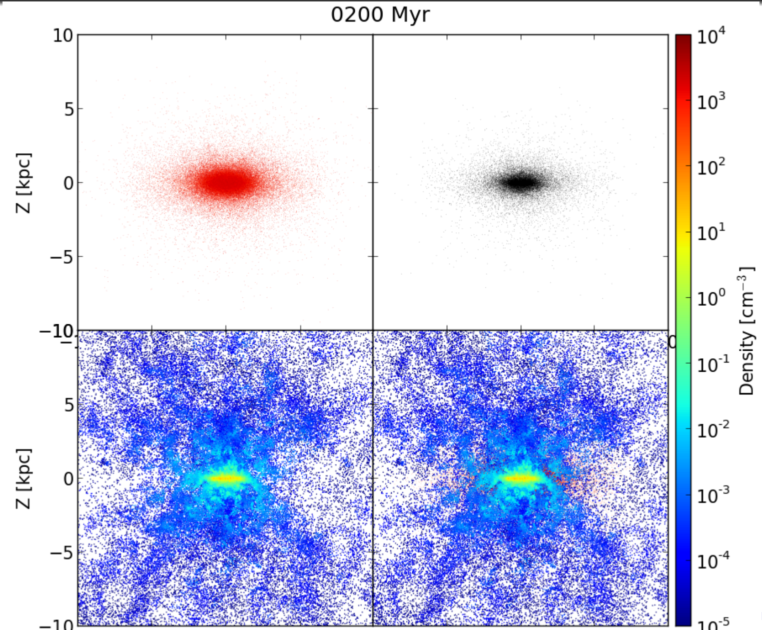

0200 Myr
Z [kpc]
Z [kpc]
10
5
0
−5
−10
Density [cm^{-3}]
10^4
10^3
10^2
10^1
10^0
10^{-1}
10^{-2}
10^{-3}
10^{-4}
10^{-5}

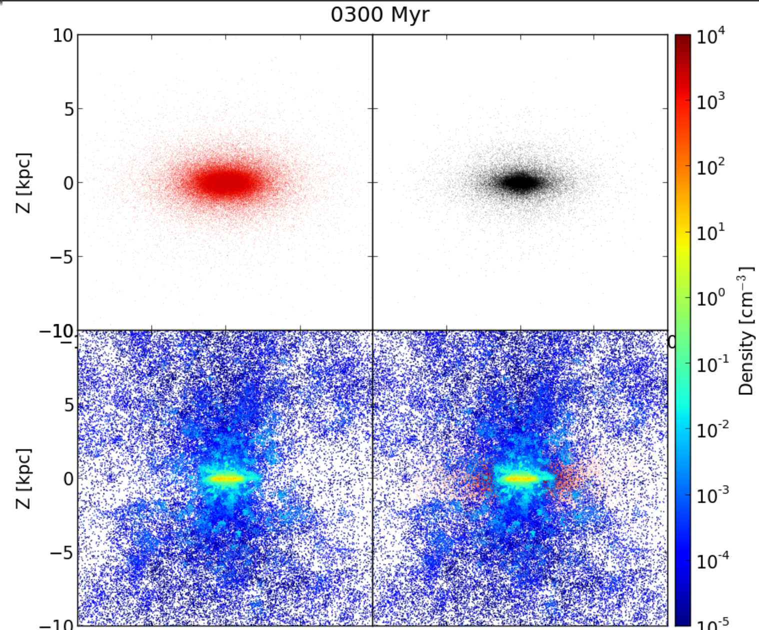
0300 Myr
10
5
0
−5
−10
Z [kpc]
10^4
10^3
10^2
10^1
10^0
10^-1
10^-2
10^-3
10^-4
10^-5
Density [cm^−3]

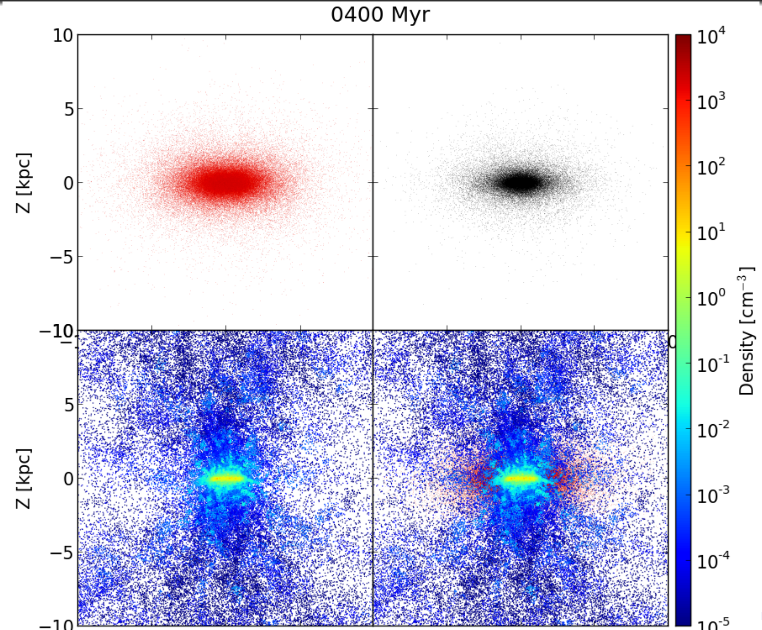
0400 Myr
10
5
0
−5
−10
Z [kpc]
10^4
10^3
10^2
10^1
10^0
10^-1
10^-2
10^-3
10^-4
10^-5
Density [cm^−3]

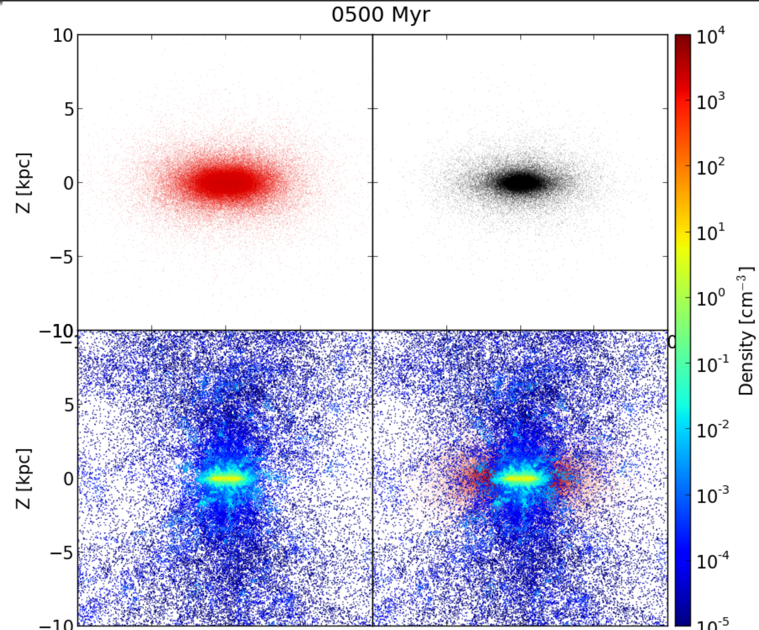
0500 Myr
Z [kpc]
10
5
0
−5
−10
Z [kpc]
5
0
−5
−10
Density [cm^{-3}]
10^4
10^3
10^2
10^1
10^0
10^{-1}
10^{-2}
10^{-3}
10^{-4}
10^{-5}

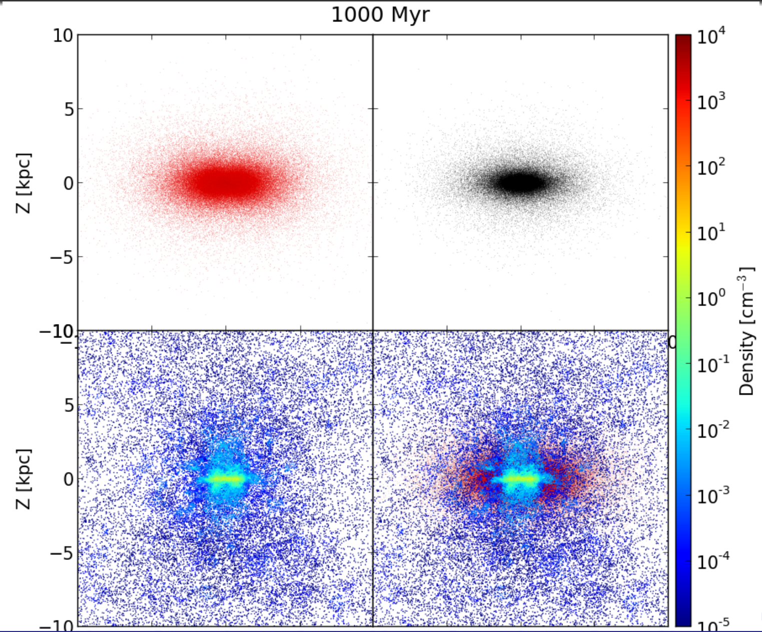
1000 Myr
10
5
0
−5
−10
Z [kpc]
Z [kpc]
10^4
10^3
10^2
10^1
10^0
10^{-1}
10^{-2}
10^{-3}
10^{-4}
10^{-5}
Density [cm^{-3}]

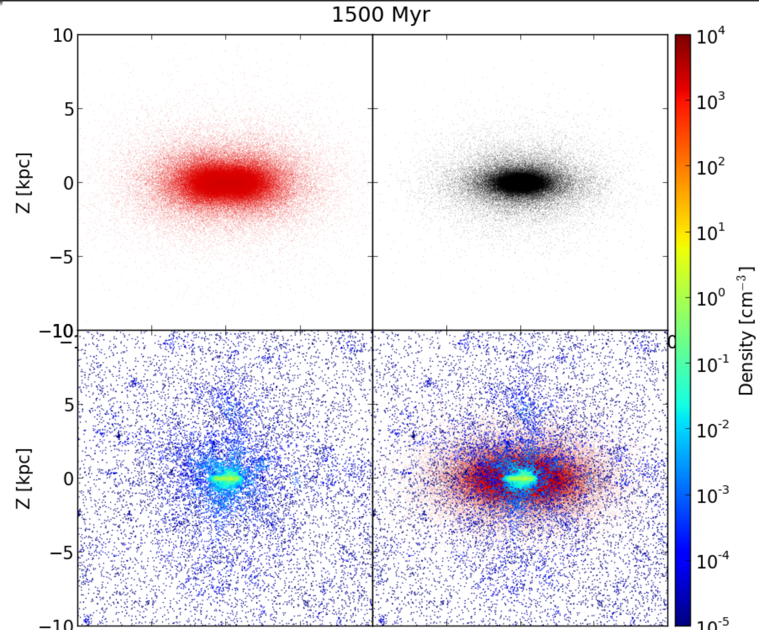
1500 Myr
10
5
0
−5
−10
Z [kpc]
Z [kpc]
10^4
10^3
10^2
10^1
10^0
10^-1
10^-2
10^-3
10^-4
10^-5
Density [cm^-3]

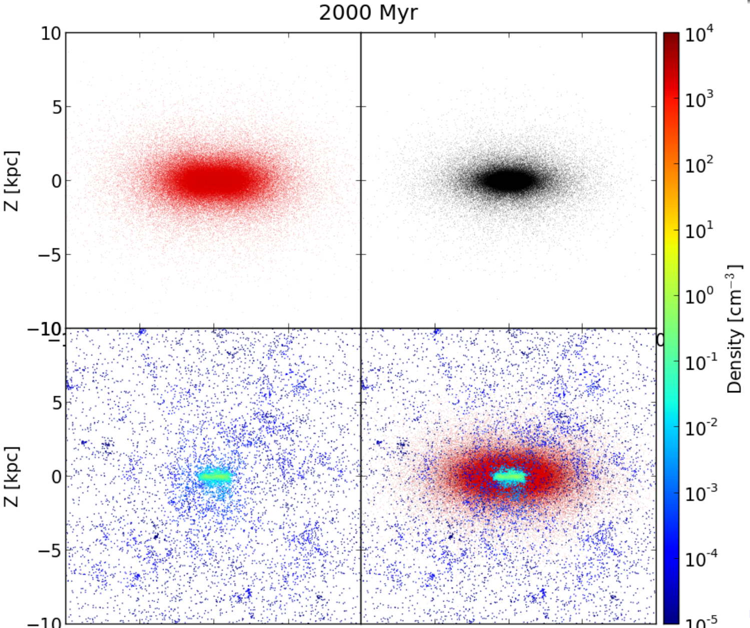
2000 Myr
Z [kpc]
Z [kpc]
10
5
0
−5
−10
Density [cm^{-3}]
10^{4}
10^{3}
10^{2}
10^{1}
10^{0}
10^{-1}
10^{-2}
10^{-3}
10^{-4}
10^{-5}

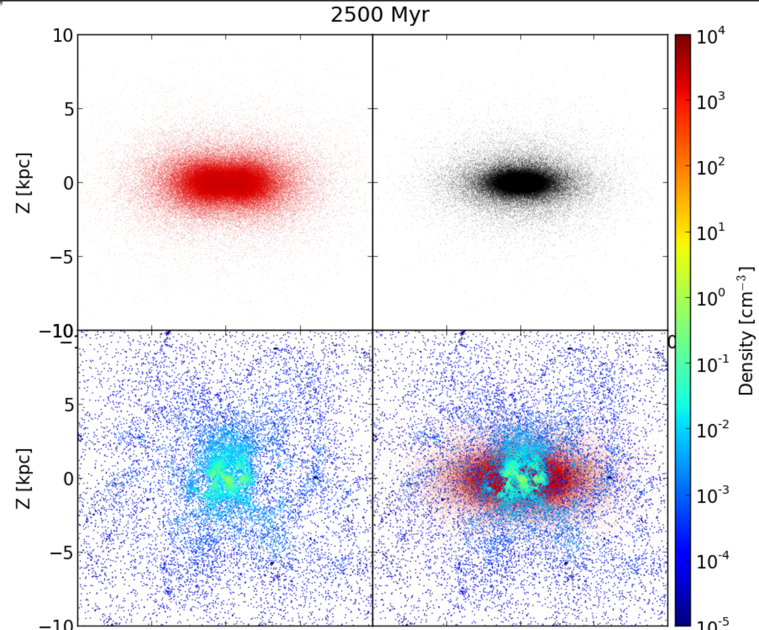
2500 Myr
Z [kpc]
10
5
0
−5
−10
Density [cm^{-3}]
10^4
10^3
10^2
10^1
10^0
10^{-1}
10^{-2}
10^{-3}
10^{-4}
10^{-5}

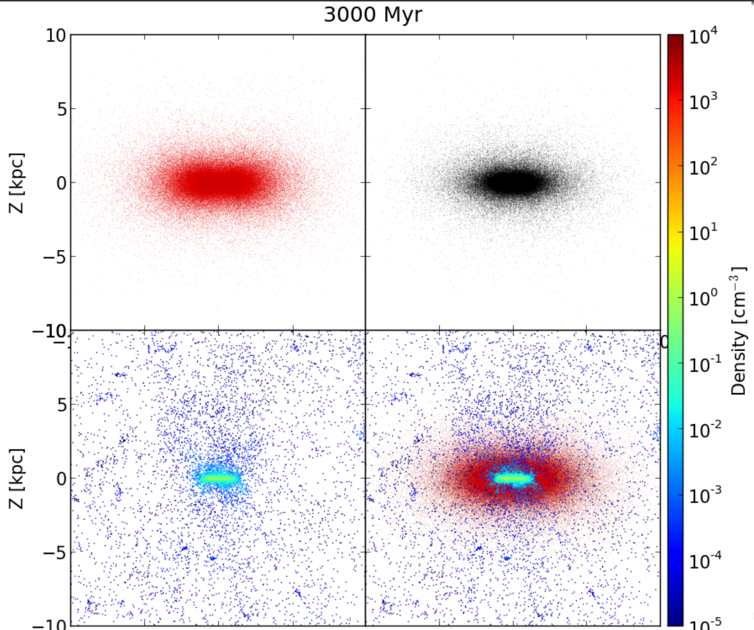
3000 Myr
10
5
0
−5
−10
Z [kpc]
10^4
10^3
10^2
10^1
10^0
10^-1
10^-2
10^-3
10^-4
10^-5
Density [cm^-3]

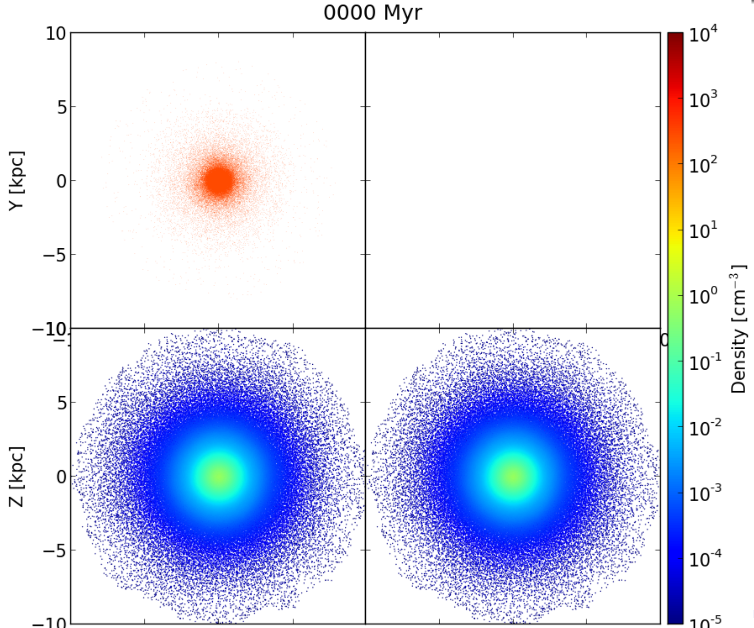
0000 Myr
Y [kpc]
Z [kpc]
10
5
0
−5
−10
Density [cm^{-3}]
10^{4}
10^{3}
10^{2}
10^{1}
10^{0}
10^{-1}
10^{-2}
10^{-3}
10^{-4}
10^{-5}

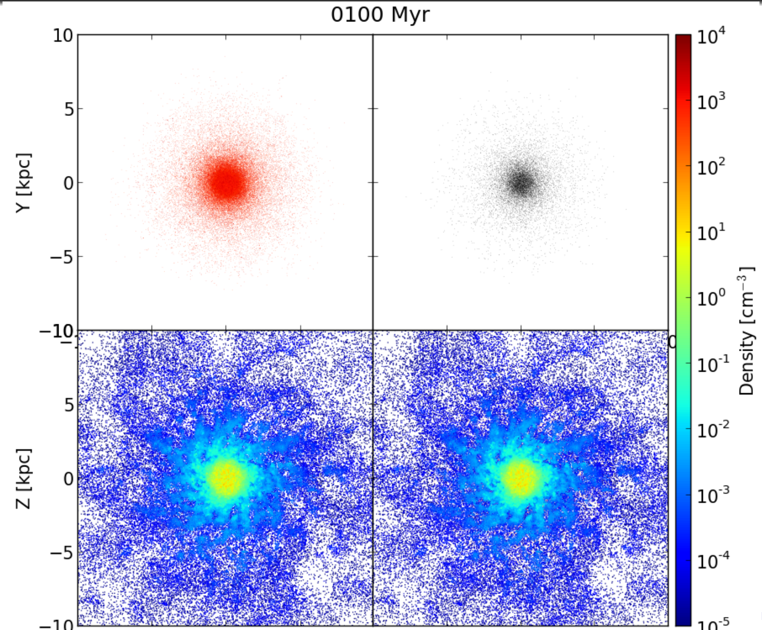
0100 Myr
10
5
0
−5
−10
Y [kpc]
Z [kpc]
Density [cm^{-3}]
10^{4}
10^{3}
10^{2}
10^{1}
10^{0}
10^{-1}
10^{-2}
10^{-3}
10^{-4}
10^{-5}

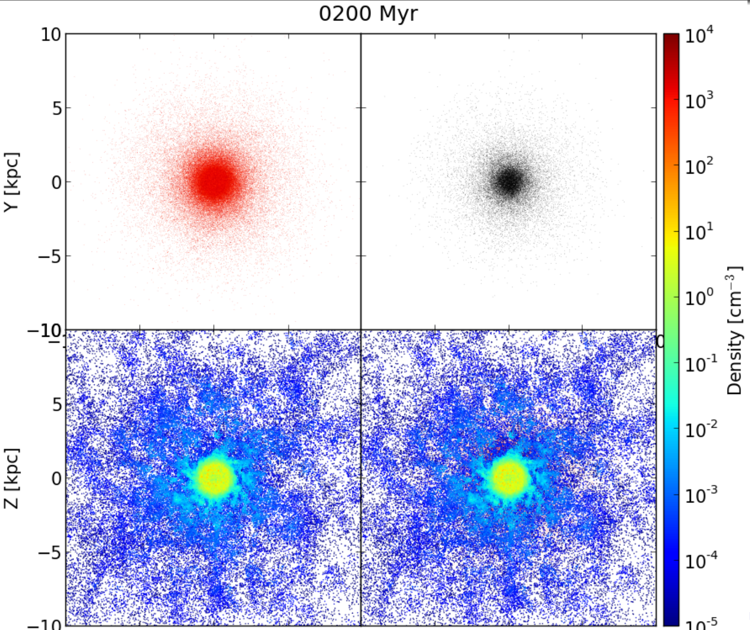
0200 Myr
10
5
0
−5
−10
Y [kpc]
Z [kpc]
10^4
10^3
10^2
10^1
10^0
10^-1
10^-2
10^-3
10^-4
10^-5
Density [cm^-3]

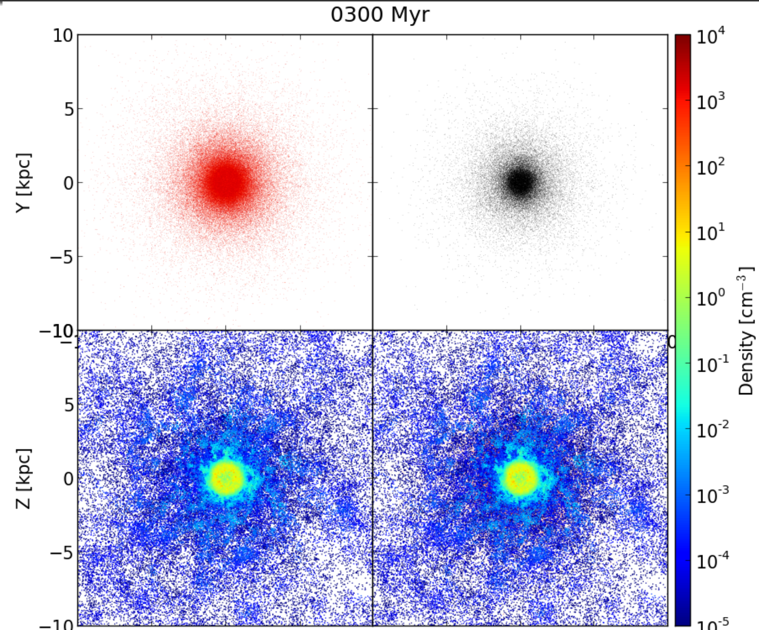
0300 Myr
Y [kpc]
Z [kpc]
10
5
0
−5
−10
Density [cm^{-3}]
10^{4}
10^{3}
10^{2}
10^{1}
10^{0}
10^{-1}
10^{-2}
10^{-3}
10^{-4}
10^{-5}

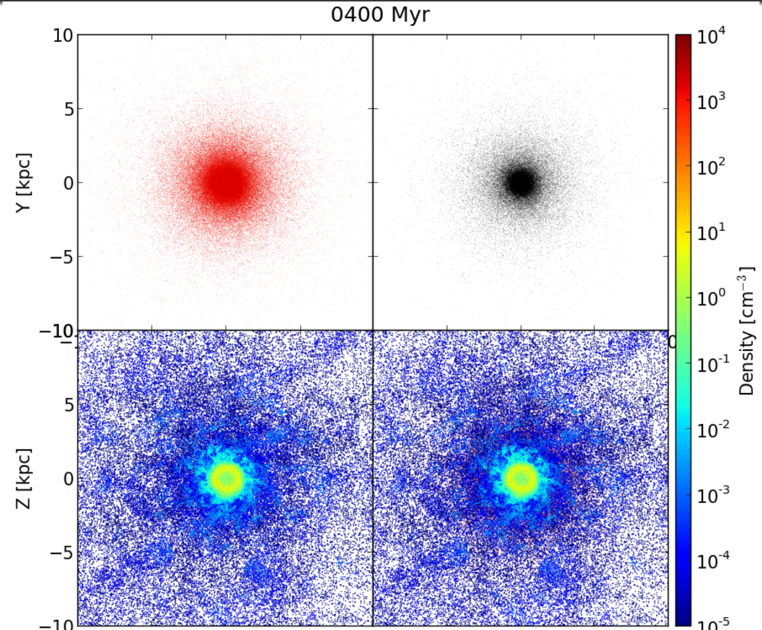
0400 Myr
10
5
0
−5
−10
Y [kpc]
5
0
−5
−10
Z [kpc]
10^4
10^3
10^2
10^1
10^0
10^{-1}
10^{-2}
10^{-3}
10^{-4}
10^{-5}
Density [cm^{-3}]

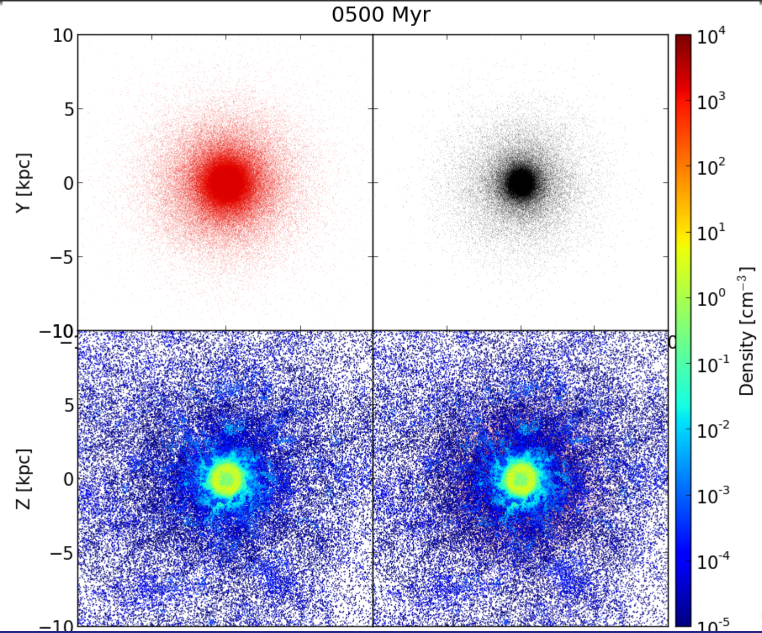

0500 Myr
Y [kpc]
Z [kpc]
10
5
0
−5
−10
10^4
10^3
10^2
10^1
10^0
10^-1
10^-2
10^-3
10^-4
10^-5
Density [cm^-3]

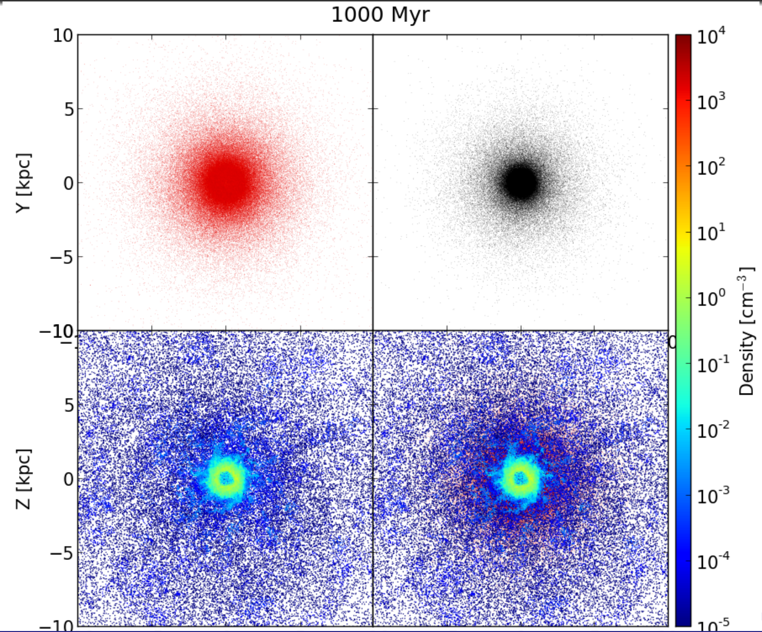
1000 Myr
10
5
0
−5
−10
Y [kpc]
Z [kpc]
10^4
10^3
10^2
10^1
10^0
10^{-1}
10^{-2}
10^{-3}
10^{-4}
10^{-5}
Density [cm^{-3}]

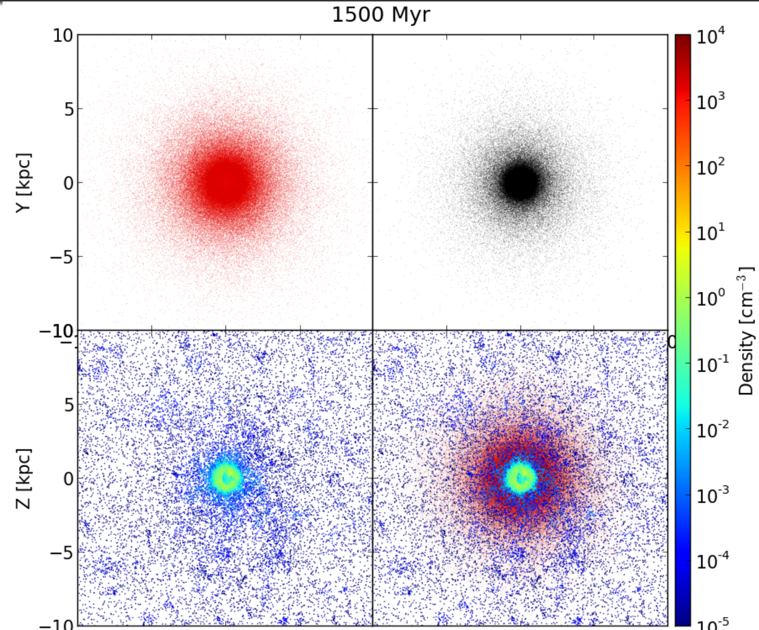
1500 Myr
Y [kpc]
Z [kpc]
10
5
0
−5
−10
Density [cm^{-3}]
10^4
10^3
10^2
10^1
10^0
10^{-1}
10^{-2}
10^{-3}
10^{-4}
10^{-5}

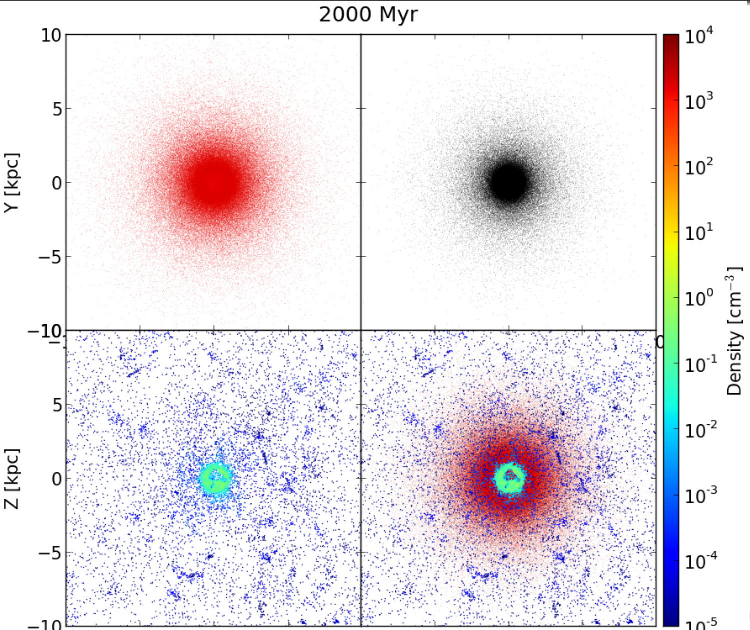
2000 Myr
Y [kpc]
Z [kpc]
10
5
0
−5
−10
Density [cm^{-3}]
10^4
10^3
10^2
10^1
10^0
10^{-1}
10^{-2}
10^{-3}
10^{-4}
10^{-5}

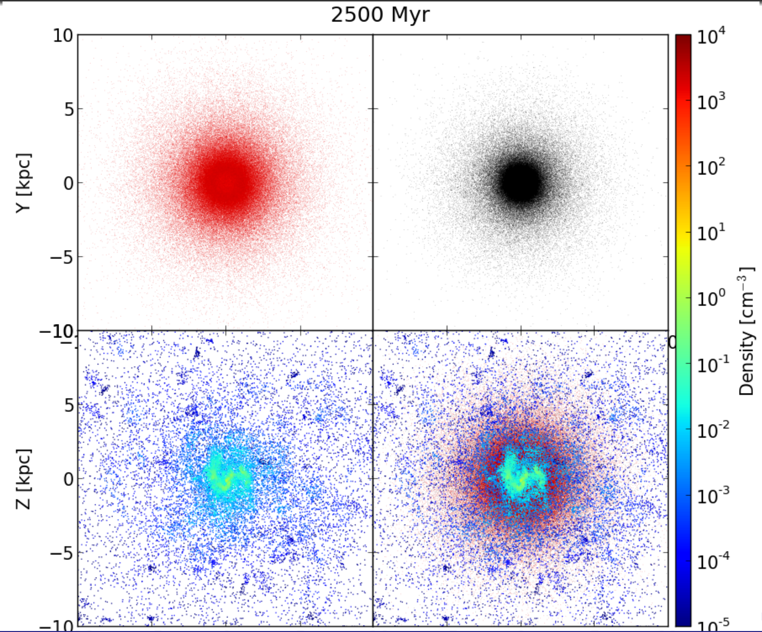
2500 Myr
10
5
0
−5
−10
Y [kpc]
Z [kpc]
10^4
10^3
10^2
10^1
10^0
10^{-1}
10^{-2}
10^{-3}
10^{-4}
10^{-5}
Density [cm^{-3}]

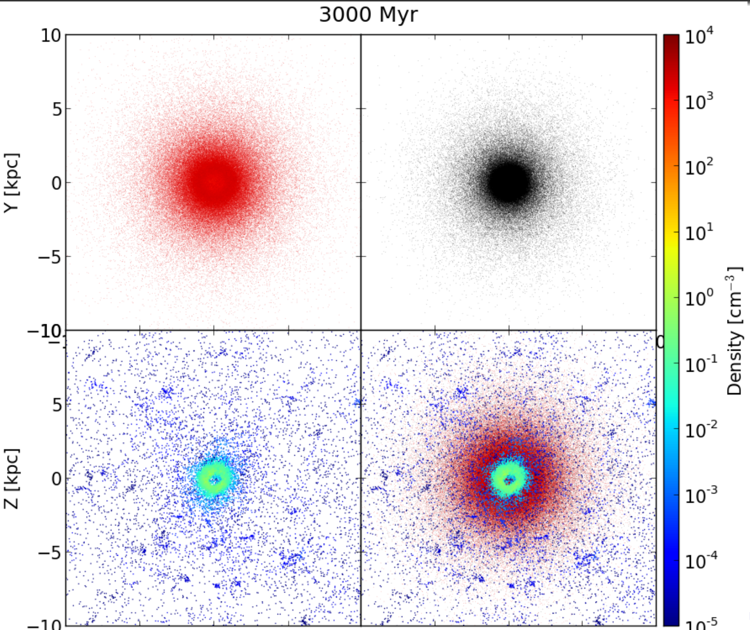
3000 Myr
10
5
0
−5
−10
Y [kpc]
Z [kpc]
10^4
10^3
10^2
10^1
10^0
10^{-1}
10^{-2}
10^{-3}
10^{-4}
10^{-5}
Density [cm^{-3}]

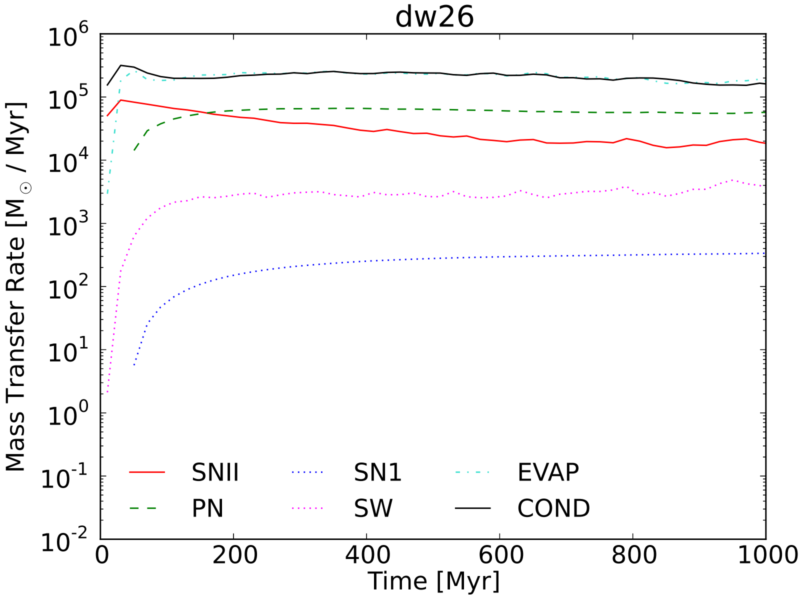
dw26
Mass Transfer Rate [M$_\odot$ / Myr]
10^6
10^5
10^4
10^3
10^2
10^1
10^0
10^{-1}
10^{-2}
0
200
400
600
800
1000
Time [Myr]
SNII
SN1
EVAP
PN
SW
COND

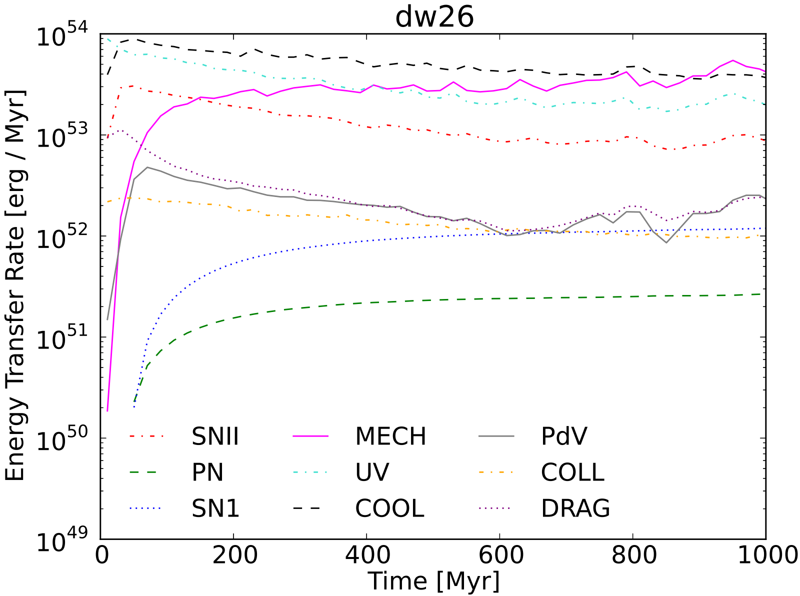
dw26
Energy Transfer Rate [erg / Myr]
Time [Myr]
10^{54}
10^{53}
10^{52}
10^{51}
10^{50}
10^{49}
0
200
400
600
800
1000
SNII
PN
SN1
MECH
UV
COOL
PdV
COLL
DRAG

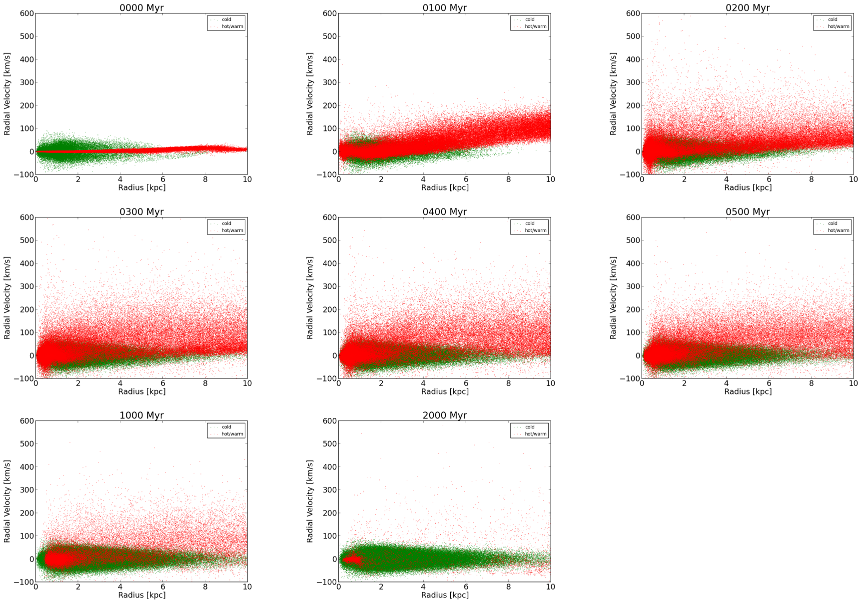
0000 Myr
0100 Myr
0200 Myr
0300 Myr
0400 Myr
0500 Myr
1000 Myr
2000 Myr
cold
hot/warm
Radial Velocity [km/s]
Radius [kpc]

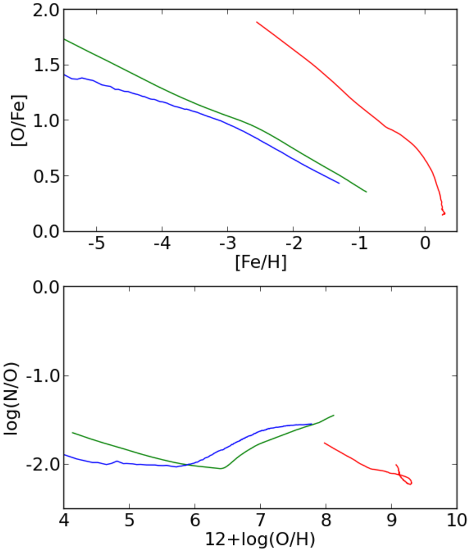
2.0
1.5
1.0
0.5
0.0
[O/Fe]
-5
-4
-3
-2
-1
0
[Fe/H]
0.0
-1.0
-2.0
log(N/O)
4
5
6
7
8
9
10
12+log(O/H)

Samland, Hensler, Theis (1997) ApJ 476, 544

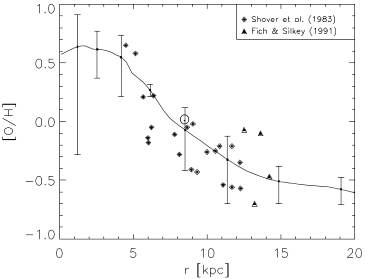

FIG. 6.—Oxygen gradient of the CM in the equatorial plane after 15×10^9 yr. The error bars indicate the local fluctuations in the model. Observational data of the sun and of H II regions (*rhombi*, *triangles*) are plotted for comparison.

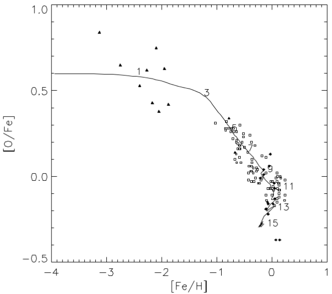

FIG. 9.—Observed [O/Fe] and [Fe/H] in comparison with a best-fit model. Abundances of disk and halo dwarf stars and B stars in the Orion association are plotted as squares, triangles, and filled rhombi, respectively. The numbers in the figure give the age (in units of 10^9 yr) to show how the abundance ratios evolve with time.

Conclusion

- The multi-phase model adds a lot additional dynamics
- Most parts are treated by analytical deliberations
- This can help to reduce the number of free parameters compared to single-phase models and less "subgrid-physics" is necessary.
- A single phase model can not reproduce typical properties of the ISM
- Multi-phase is necessary for modelling the characteristic chemical evolution of hot/warm gas and cold clouds. This is a strong motivation for favouring a multi-phase approach.